Superplasticity in a 7055 aluminum alloy processed by ECAE and subsequent isothermal rolling

I. Nikulin [a], R. Kaibyshev [a,*], T. Sakai [b]

[a] *Institute for Metals Superplasticity Problems, Khalturina 39, Ufa 450001, Russia*
[b] *Department of Mechanical Engineering and Intelligent Systems, UEC Tokyo, The University of Electro-Communications, 182-8585, Japan*

Abstract

The superplastic properties and microstructural evolution of a 7055 aluminum alloy was examined in tension at temperatures ranging from 300 to 450 °C and strain rates ranging from 2.7×10^{-5} to 5.6×10^{-2} s^{-1}. A refined microstructure with an average grain size of ~1.4 μm and a portion of high-angle grain boundaries (HAGBs) of ~67% was produced in sheets by equal channel angular extrusion (ECAE) followed by isothermal rolling (IR) at 250 °C. The alloy exhibited a maximum elongation-to-failure of ~820% at a temperature of 450 °C and an initial strain rate of 5.6×10^{-3} s^{-1}. Superplastic elongation of ~670% was recorded at strain rates higher than 10^{-2} s^{-1}, where the strain rate sensitivity coefficient was around 0.44. The relationship between superplastic ductilities and microstructure stability was analyzed. It was shown that increasing the portion of HAGBs by IR results in enhancement of superplastic properties.

Keywords: Aluminum alloy; Fine-grained structure; Equal channel angular extrusion; Rolling; Superplasticity; Microstructure

1. Introduction

Superplastic forming (SPF) of metal sheets is used for the fabrication of components with good surface quality and excellent tolerance [1,2]. The manufacture of complex parts for the aerospace industry by gas blow forming requires the SPF regime in which aluminum alloys are extremely resistant to neck formation under biaxial tension and exhibit ductilities over ~500% [2]. Grain refinement resulting from warm working and recrystallization treatment of aluminum alloys is an essential prerequisite for superplasticity [2,3]. SPF of aluminum alloys is carried out at forming rates below $\sim 10^{-3}$ s^{-1} [2,3] so that the forming times are generally ~40 min for each component or even longer. These slow forming rates restrict the commercial application of SPF. Shorter forming time can provide a significant increase in economic efficiency of the SPF technique.

Recent studies [4–6] showed that high strain rate superplasticity (HSRS) can be achieved in aluminum alloys through extensive grain refinement via ECAE. It is known [2–4] that the strain rate associated with highest superplastic ductility varies inversely with the grain size raised to a power of ~2 or ~3; the superplastic regime is displaced to higher strain rates when the grain size is reduced. Conventional thermomechanical processing (TMP) of aluminum alloys results in grain size ranging from 6 to 10 μm [2]. In contrast, ECAE provides the formation of uniform ultrafine grained structure with an average size of 1 μm or even less [4–7]. It is worth noting that merely achieving a finer grain size is not sufficient to guarantee that the aluminum alloy exhibits superplasticity at increased strain rates, since the grain size needs to remain stable throughout the deformation process [2,3]. This microstructural stability can be provided by Zr and/or Sc, which produce nanoscale dispersoids acting as an effective pinning agent to hinder the migration of grain boundaries. HSRS takes place in ECAE processed aluminum alloys containing a dispersion of nanoscale precipitates [4–7]. The resulting microstructures produced by ECAE in these aluminum alloys are very uniform to avoid extensive grain growth under superplastic conditions [3,7]. Therefore, high superplastic ductilities at around 10^{-2} s^{-1}

* Corresponding author.
E-mail address: rustam@anrb.ru (R. Kaibyshev).

[4–7], which is the highest strain rate being useful in SPF process, can be achieved in ultrafine grained aluminum alloy containing a high fraction of nanoscale dispersoids, via severe plastic deformation techniques.

Samples produced by ECAE are generally in the form of rods having square or circular cross-sections, which cannot be used directly in industrial SPF forming operations where the material is required to be in the form of thin sheets. It was recently shown in [8,9] that aluminum alloys with ultrafine grain structure can be produced as sheets through combination of ECAE and rolling. Billets in the form of plates having rectangular cross-section are best suited to roll thin sheets. The authors of [10] demonstrated that ECAE with rectangular shape of channels was readily carried out to produce fine-grained aluminum alloy in the form of plates. Therefore, the ECAE with rectangular shape of channels followed by rolling is considered as an advanced technique for the fabrication of thin superplastic aluminum sheets.

The present study was initiated to demonstrate the feasibility of this technique for attaining HSRS in a 7055 aluminum alloy, called 7055 Al hereafter. This age-hardenable alloy, used for airplane structures with highest strength [11,12], has usually a limited formability at room temperature that makes difficult to fabricate thin sheets due to extensive edge cracking developed by cold rolling [11,12]. To overcome this limitation, isothermal rolling (IR) following ECAE was applied to produce thin sheets of 7055 Al.

2. Material and experimental procedure

7055 Al with a chemical composition of Al–8.2% Zn–2.1% Mg–2.2% Cu–0.2% Zr–0.09% Mn–0.09% Fe–0.07% Si–0.04% Ni–0.02% Ti–0.08% Cr (all in wt%) was manufactured by direct chill casting and then homogenized at 470 °C for 24 h and quenched into water. The alloy was annealed at 410 °C for 8 h, followed by slow cooling in a furnace. Plates with a rectangular cross-section of 125 mm × 25 mm and a height of 125 mm (Fig. 1) were machined from the central part of the ingot parallel to the major axis. These plates were deformed by ECAE at

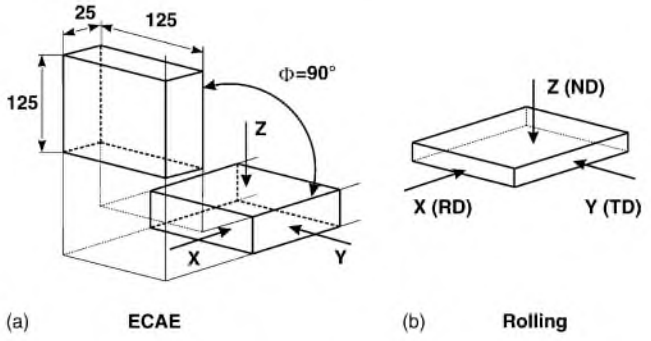

Fig. 1. Schematic illustration of: (a) rectangular plate for ECAE and (b) subsequent rolling.

250 °C. An isothermal die with a rectangular cross-section of 125 mm × 25 mm and a channel angle Φ of 90° had a horizontal L-shaped configuration (Fig. 1a) [10]. The angle Ψ, which represents the outer arc of the curvature where the two parts of the channel intersect, was equal to ~1°. Deformation through this die produced an imposed strain of ~1 in each passage [10]. The plates were pressed 10 times with approximate total accumulated strain of ~10 without any rotation of the plate between successive pressings, i.e. route A was used [10]. The pressing speed was approximately 3 mm s^{-1}.

The as-pressed plates were ground parallel to the extrusion direction and 5 mm from each side was removed to give plates with flat parallel surfaces without defective layers. These plates with dimensions of 115 mm × 115 mm × 15 mm were heated to 250 °C and then rolled to a final thickness of 1.7 mm, giving a total reduction of 85% in seven passes. The *X*, *Y* and *Z* planes correspond to the planes perpendicular to the rolling (RD), transverse (TD) and normal (ND) directions, respectively, as shown in Fig. 1b. A 6-high mill with isothermal internal rollers of 65 mm in diameter and 250 mm in length was used. The internal rollers were heated and kept at 250 °C during rolling.

Tensile specimens of 6 mm gauge length and 1.4 mm × 3 mm cross-section were machined from the resulting thin sheets; the gauge lengths were parallel to the RD. These samples were tensioned to failure in the temperature interval of 300–450 °C at strain rates ranging from 2.7×10^{-5} to 5.6×10^{-2} s^{-1}. Each sample was held at the testing temperature for about 30 min in order to reach thermal equilibrium. The values of the strain rate sensitivity *m* were determined by strain rate jump tests [2,3]. The other details of the mechanical tests were described in previous reports [12,13].

Microstructural examination was carried out in parallel sections of the *Y*-plane, i.e. (RD)–(ND) sections of the rolled plate. Microstructural changes and cavitation during superplastic deformation were examined in parallel sections of the *Z*-plane, i.e. (RD)–(TD) sections. The areas within 5 mm of the fracture surface were analyzed to examine cavitation. The methods of optical metallography, cavitation studies and electron backscattering diffraction (EBSD) analysis were described in previous papers in detail [6,12–14]. The misorientations of (sub)grain boundaries were determined using a JEOL JSM-840 SEM fitted with an automated EBSD pattern collection system provided by Oxford Instruments, Ltd.

3. Experimental results

3.1. Microstructures after ECAE and isothermal rolling

Typical EBSD maps and the distribution of boundary misorientations after ECAE and IR following ECAE are presented in Figs. 2 and 3, respectively. Black and white lines indicate the high-angle grain boundaries (HAGBs)

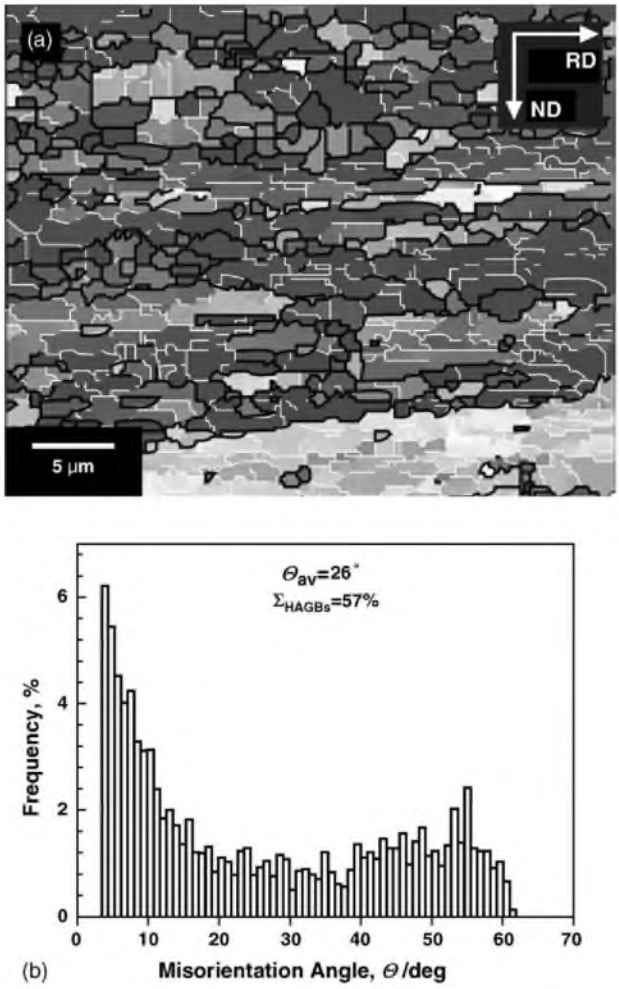

Fig. 2. Microstructure of the 7055 Al after ECAE processing with a total strain of ~10 at 250 °C. (a) Typical EBSD map and (b) misorientation distribution.

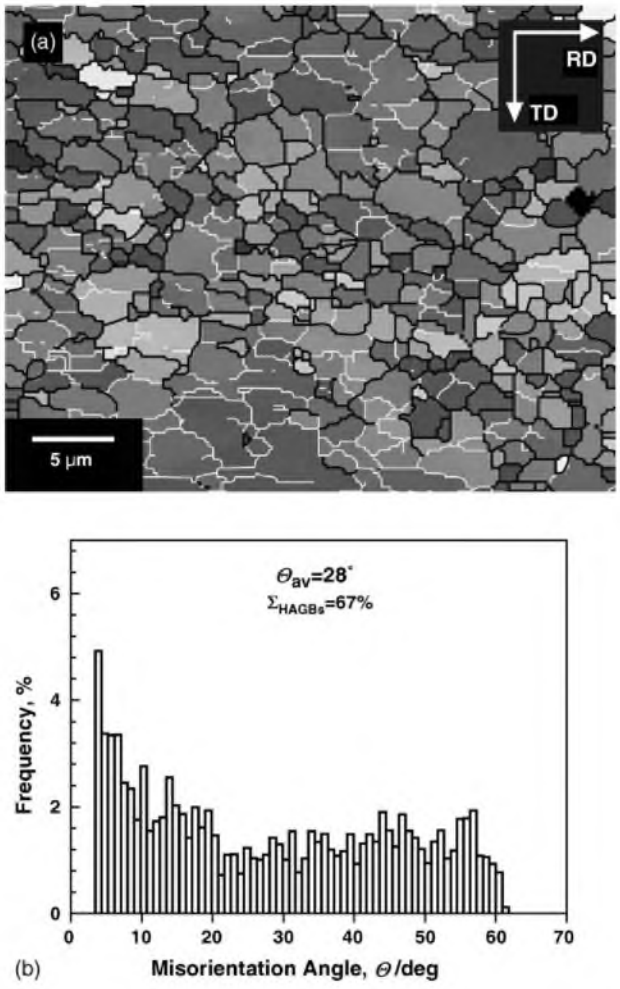

Fig. 3. Initial microstructure of the 7055 Al after ECAE to $\varepsilon \sim 10$ followed by isothermal rolling with a total reduction of 85% at 250 °C. (a) Typical EBSD map and (b) misorientation distribution.

($\geq 15°$) and low-angle grain boundaries (LAGBs) (3–15°), respectively. It is clearly seen in Fig. 2 that a non-uniform microstructure consisting of two components is developed in the plate even after 10 passes of ECAE. The one consists of newly developed grains with HAGBs, the average size of which is ~2 μm in *X*-direction and ~1 μm in *Z*-direction. The other type comprises highly elongated initial grains having a well-defined subgrain structure. Size of subgrains outlined by LAGBs is ~3.3 μm in *X*-direction and ~1.1 μm in *Z*-direction. The fraction of HAGBs is about 57%.

Subsequent IR resulted in the formation of a more uniform microstructure, as shown in Fig. 3. The fraction of HAGBs is ~67% (Fig. 3b), which is quite near to 70% in conventional granular structure [15]. The average misorientation $\theta \approx 28°$ is close to that of 30° in strain-induced grain structures in fcc materials processed by severe plastic deformation [16]. In addition, IR following ECAE reduced slightly the average grain size to 1.4 μm. The grain aspect ratio (AR), defined as the ratio of the grain dimension in the rolling direction to that in the transverse direction, is ~1.3. Subgrain growth took place slightly in unrecrystallized regions; the longitudinal and transversal size of subgrains is ~3.3 and ~1.9 μm, respectively.

3.2. Superplastic behavior

The typical true stress–true strain curves in the temperature interval 300–450 °C at an initial strain rate of $1.4 \times 10^{-3}\,s^{-1}$, and at a fixed temperature of 425 °C and strain rates ranging from 2.7×10^{-4} to $5.6 \times 10^{-3}\,s^{-1}$ are shown in Fig. 4a and b, respectively. Extensive strain hardening takes place at low strains ($\varepsilon \leq 0.5$). At $T \geq 400$ °C and $\dot{\varepsilon} \leq 1.4 \times 10^{-3}\,s^{-1}$, weak strain softening following a stress maximum occurs until failure and roughly uniform deformation takes place within gauge lengths (Fig. 5). Pseudo-brittle fracture associated with cavitation restricts superplastic ductilities at the present conditions. It is worth noting that cavitation may yield an apparent strain softening at high strains

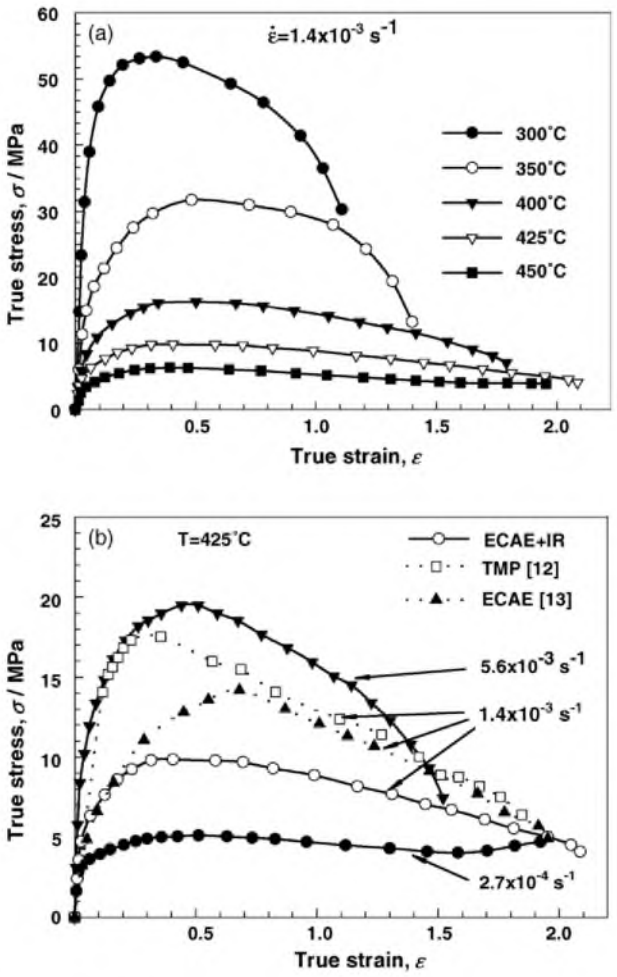

Fig. 4. True stress–true strain curves of 7055 Al subjected to ECAE + IR. (a) The temperature dependence at an initial strain rate of $1.4 \times 10^{-3}\ s^{-1}$ and (b) the strain rate dependence at 425 °C. The data for 7055 Al subjected to conventional TMP [12] and ECAE [13] are inserted for comparison.

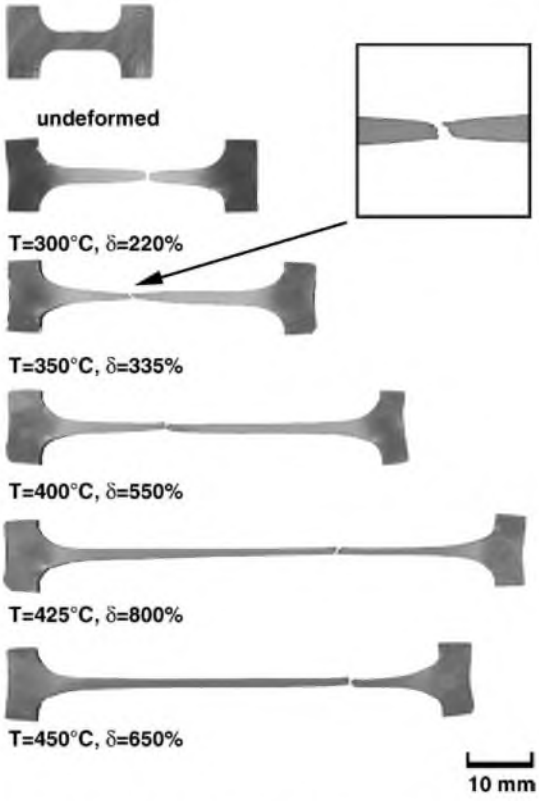

Fig. 5. Appearance of samples pulled to failure at $\dot{\varepsilon} = 1.4 \times 10^{-3}\ s^{-1}$ and at various temperatures. The zoomed image of the sample crack area shows that crack propagation occurs at an angle of ~45° relative to the tension axis at 350 °C.

through decreasing the sample cross-section [2]. At low temperatures below 400 °C and/or higher strain rates above $1.4 \times 10^{-3}\ s^{-1}$, the rapid strain softening observed after a stress peak can be attributed to strain localization due to necking over the gauge lengths (Fig. 5). Notably the present aluminum alloy subjected to ECAE followed by IR exhibits the weakest strain dependence of flow stress in superplastic conditions in comparison with the 7055 Al subjected to ECAE [13] or TMP [12] (Fig. 4b). In general, at $T \geq 400$ °C and $\dot{\varepsilon} \leq 1.4 \times 10^{-3}\ s^{-1}$, the peak stresses of the present alloy were less than those for the 7055 Al processed by ECAE [13] or conventional TMP [12] by a factor of ~1.4 and ~2, respectively, as can be seen in Fig. 4b.

Fig. 6 shows the flow stresses taken at $\varepsilon \sim 0.34$, the strain rate sensitivity, m, and the elongation-to-failure, δ, versus strain rate. It is clearly seen that at $T \geq 400$ °C, the σ–$\dot{\varepsilon}$ curves show a sigmoidal shape, i.e. three regions of superplastic deformation can be identified [2,3]. The maximum values of m and δ appear in the second region, where $m \geq 0.4$ and $\delta \geq 400\%$. The optimum strain rate region for superplasticity [2,3] tends to shift to higher strain rates with increasing temperature from 300 to 450 °C. At 300 °C, the maximum elongation to failure of 435% and $m \sim 0.41$ is observed at a strain rate of $5.6 \times 10^{-5}\ s^{-1}$. At 450 °C, the well-defined maximum elongation of 820% is observed at $5.6 \times 10^{-3}\ s^{-1}$, while the highest m value of 0.63 occurs at around $10^{-3}\ s^{-1}$. It should be also noted that at 450 °C, the m value of 0.44 and an elongation of 670% appears at strain rates higher than $10^{-2}\ s^{-1}$. This may suggest the occurrence of HSRS in the 7055 Al subjected to ECAE followed by isothermal rolling.

Fig. 7 shows changes in m with strain at various temperatures. At temperatures below 400 °C, the m values tend to decrease with strain, while they are essentially unchanged at higher temperatures. It is known [6,13] that combinations of high values of $m \geq 0.5$ and rather small strain softening at $T \geq 400$ °C can result in high resistance to the neck development thus providing high tensile elongations.

At $\dot{\varepsilon} = 1.4 \times 10^{-3}\ s^{-1}$, the sharp increase in δ value from ~300 to ~800% occurs with an increase in temperature from 350 to 425 °C (Fig. 8). Further temperature increase leads to a decrease in superplastic ductility (Fig. 8). To evaluate the reproducibility of experimental data, at least three samples for

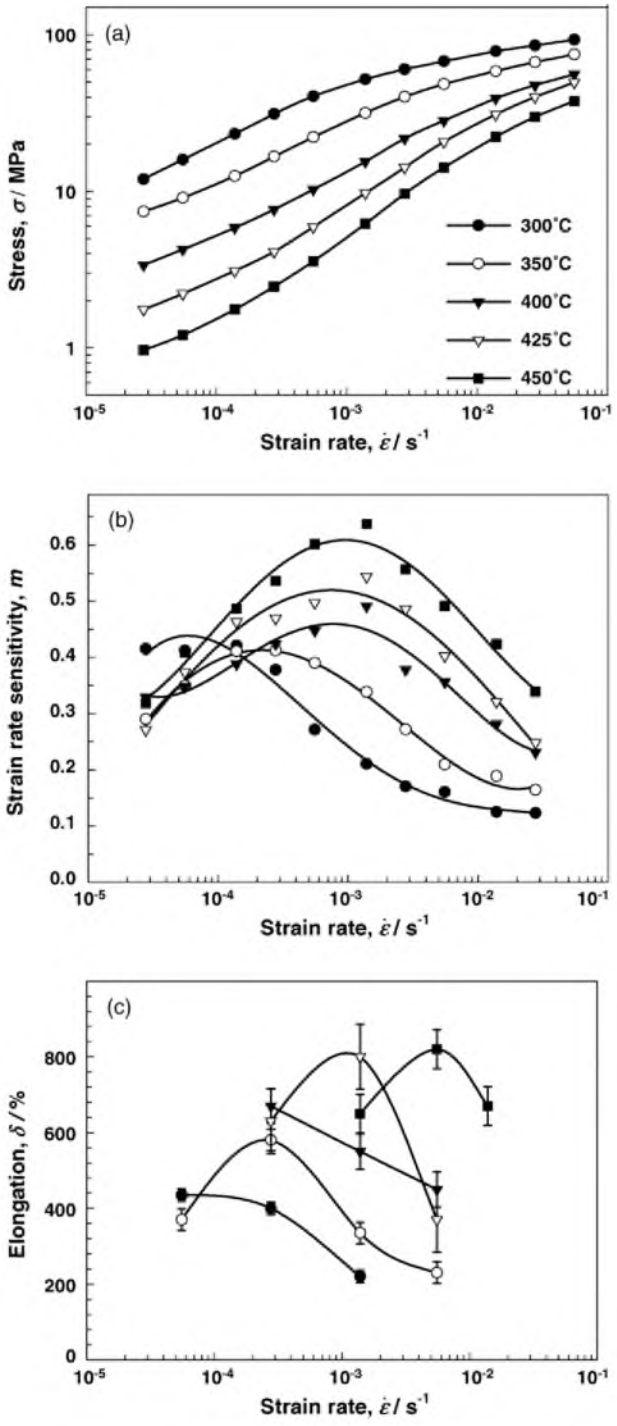

Fig. 6. Strain rate dependence of (a) flow stress, σ, taken at $\varepsilon \sim 0.34$, (b) coefficient of strain rate sensitivity, m, taken at $\varepsilon \sim 0.34$ and (c) elongation-to-failure, δ, for 7055 Al processed by ECAE + IR. The symbols of temperature defined in (a) are also valid for (b) and (c).

each testing temperature were pulled to failure at an initial strain rate of $\dot{\varepsilon} = 1.4 \times 10^{-3}\,s^{-1}$ in the temperature interval 300–450 °C (Fig. 8). It is seen that 7055 Al subjected to ECAE and subsequent IR exhibits a good reproducibility of superplastic properties (Fig. 8).

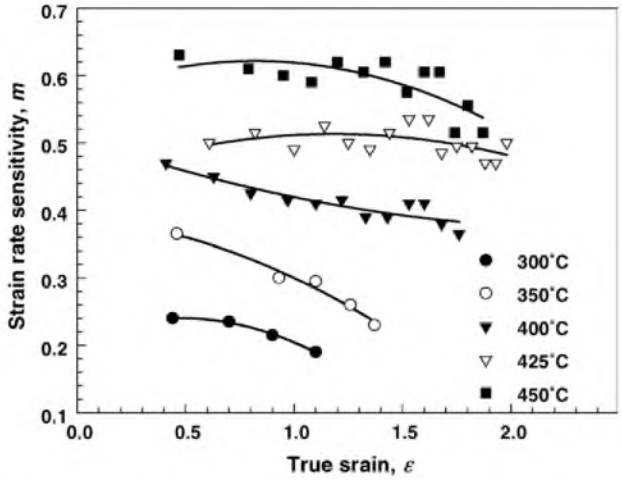

Fig. 7. Variation of the strain rate sensitivity coefficient, m, with strain.

3.3. Microstructural evolution

3.3.1. Microstructural evolution during static and dynamic annealing

The microstructure evolution of the 7055 Al subjected to ECAE and subsequent IR during static and dynamic annealing was studied in grip and gauge sections, respectively (Fig. 9; Table 1). The microstructure of the ECAE processed 7055 Al [13] after static annealing is also presented in Fig. 9a for comparison. Grain sizes observed after static annealing, L_s, dynamic annealing, L_d, and the corresponding grain aspect ratios, AR_s and AR_d, are summarized in Table 1. The ultrafine grains produced by ECAE followed by IR at 250 °C are essentially stable during static annealing at $T \leq 350$ °C, while static annealing at $T \geq 400$ °C leads to remarkable grain growth (Fig. 9b) and a decrease in AR_s (Table 1); static annealing increases the uniformity of grain structure evolved in the alloy processed by ECAE and subsequent IR. This result is in contrast with the data on microstructural evolution

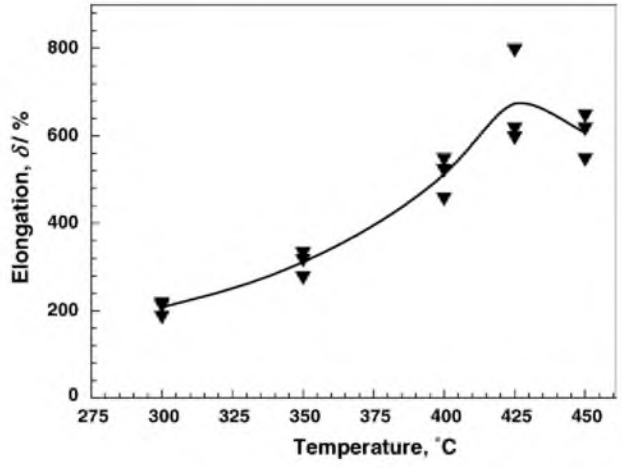

Fig. 8. Temperature dependencies of the elongation to failure at an initial strain rate of $\dot{\varepsilon} = 1.4 \times 10^{-3}\,s^{-1}$.

Table 1
Average grain size, L_s and L_d, and the grain aspect ratios, AR_s and AR_d after static annealing and superplastic deformation, respectively, of 7055 Al strained up to failure at a strain rate of $1.4 \times 10^{-3}\,s^{-1}$ and temperatures ranging from 300 to 450 °C

	T (°C)				
	300	350	400	425	450
Local strain in gauge sections (the equivalent time of static annealing in grip sections, h)	$\varepsilon = 1.1$ (1.01)	$\varepsilon = 1.4$ (1.22)	$\varepsilon = 1.8$ (1.64)	$\varepsilon = 2.1$ (2.26)	$\varepsilon = 1.9$ (2.01)
L_s (μm)[a]	2.1/1.1	2.3/1.2	5.6/4.5	5.6/5.2	7.9/7.7
AR_s	1.91	1.92	1.24	1.07	1.02
L_d (μm)[a]	2.3/1.3	2.9/1.8	7.7/5.3	11.4/9.0	12.9/9.7
AR_d	1.77	1.61	1.45	1.27	1.33

[a] Numerator and denominator are grain sizes measured in the longitudinal and transverse directions, respectively.

for the ECAE processed 7055 Al [13], where a non-uniform structure introduced by ECAE remains stable after static annealing, as shown in Fig. 9a.

Under dynamic annealing conditions, no substantial grain growth takes place at $T \leq 350$ °C, while rather large values of AR_d suggest some contribution of dislocation glide to the total deformation [2,3]. Such a large AR_d value may be indicative of decreased contribution of grain boundary sliding (GBS) to total elongation which is supported by a decrease in the m value with strain at these temperatures (Fig. 7) [2,3]. On the other hand, a significant grain growth taking place at $T \geq 400$ °C results in the formation of a very uniform microstructure consisting of equiaxed grains (Fig. 9c). A decrease in AR_d with increasing temperature (Table 1) suggests increased contribution of GBS to total elongation [2,3]. Thus, at $T \geq 400$ °C, the initial rapid strain hardening can be associated with strain-enhanced grain growth [2]; increased uniformity of equiaxed grain structure can facilitate the occurrence of GBS. As a result, no significant variation of m with strain is expected to take place at these temperatures (Fig. 7).

3.3.2. *Cavitation and fracture*

Remarkable cavitation was found to occur at $T \geq 400$ °C. The average size of cavities, A, the cavity aspect ratio, CAR and the volume fraction of porosity, V are summarized in Table 2. A, CAR and V values increase with increasing temperature (Table 2). Most cavities grow mainly along the tensile direction and have an irregular and jagged shape suggesting the operation of a plasticity-controlled cavity growth mechanism [2], as can be seen in Fig. 10. It is seen (Fig. 10b and c) that most of the cavities are chained in tensile direction. Cavity linkage takes place in the transverse direction leading to the initiation of the pseudo-brittle fracture [2], which occurs almost without necking (Fig. 5). In the temperature range 300–350 °C, in contrast, plastic deformation induces only limited cavitations. The porosity volume fraction measured was less than the accuracy of the standard point-count technique used [6,12,13]. The failure accompanied by an unstable plastic flow results from the crack propagation at an angle of ~45° to the tension axis (Fig. 5).

Table 2
Average cavity size, A, coefficient of cavity aspect ratio, CAR and porosity volume fraction, V, of 7055 Al strained up to failure at various temperatures and $\dot{\varepsilon} = 1.4 \times 10^{-3}\,s^{-1}$

	T (°C)		
	400	425	450
A (μm)[a]	2.0/2.0	6.3/4.6	11.4/6.6
CAR	1	1.4	1.7
V (%)	1.7	4.3	8.5

[a] Numerator and denominator represent cavity sizes measured in the longitudinal and transverse directions, respectively.

The samples subjected to ECAE and IR exhibit lower cavitation and smaller cavity size compared to the ECAE processed 7055 Al [13] or the TMPed alloy [12]. The lower cavitation tendency in the present material can be attributed to the finer grain sizes and enhanced uniformity of microstructure comparing with those for the alloy processed by only ECAE or TMP [12,13]. Lower flow stresses associated with smaller grain size (Fig. 4b) increases the critical size of a cavity, thereby making the cavity nucleation event more difficult [17]. In addition, the uniform structure consisting of equiaxed finer grains in the present material can be more beneficial for GBS accommodation under superplastic deformation [2,3]. When GBS cannot frequently take place, stress concentration at the grain boundary may cause the development of cavitation due to a plasticity-controlled cavity growth mechanism [2,17]. Thus, the 7055 Al processed by ECAE and IR should show larger elongation before cavity initiation, because the rate of cavity growth in this material is slowed down due to the fine and uniform microstructure produced by static annealing prior to superplastic deformation.

4. Discussion

The present study demonstrates that the two-step processing consisting of ECAE followed by IR is capable to fabricate thin sheets of 7055 Al with an ultrafine grained structure. The ECAE at 250 °C to a total strain of ~10 is a way to produce plates containing a partly recrystallized grain structure with a grain size of ~1.5 μm. Subsequent IR increases the proportion of HAGBs from 57 to 67% in the final structure. This leads to transformation of the recrystallization mode from discontinuous static recrystallization (DSRX) to a

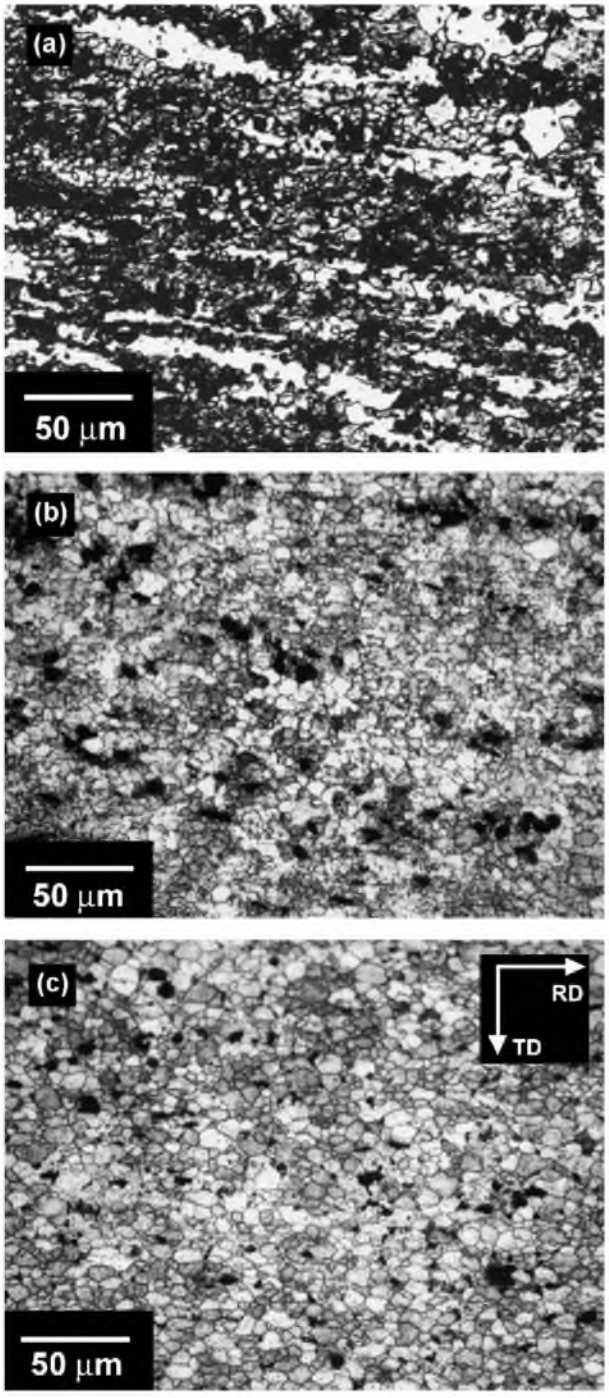

Fig. 9. Microstructures evolving during superplastic deformation: (a) grip section at 400 °C for sample processed by ECAE [13], (b) grip section and (c) gauge section at 400 °C and $1.4 \times 10^{-3}\,s^{-1}$ for samples processed by ECAE + IR.

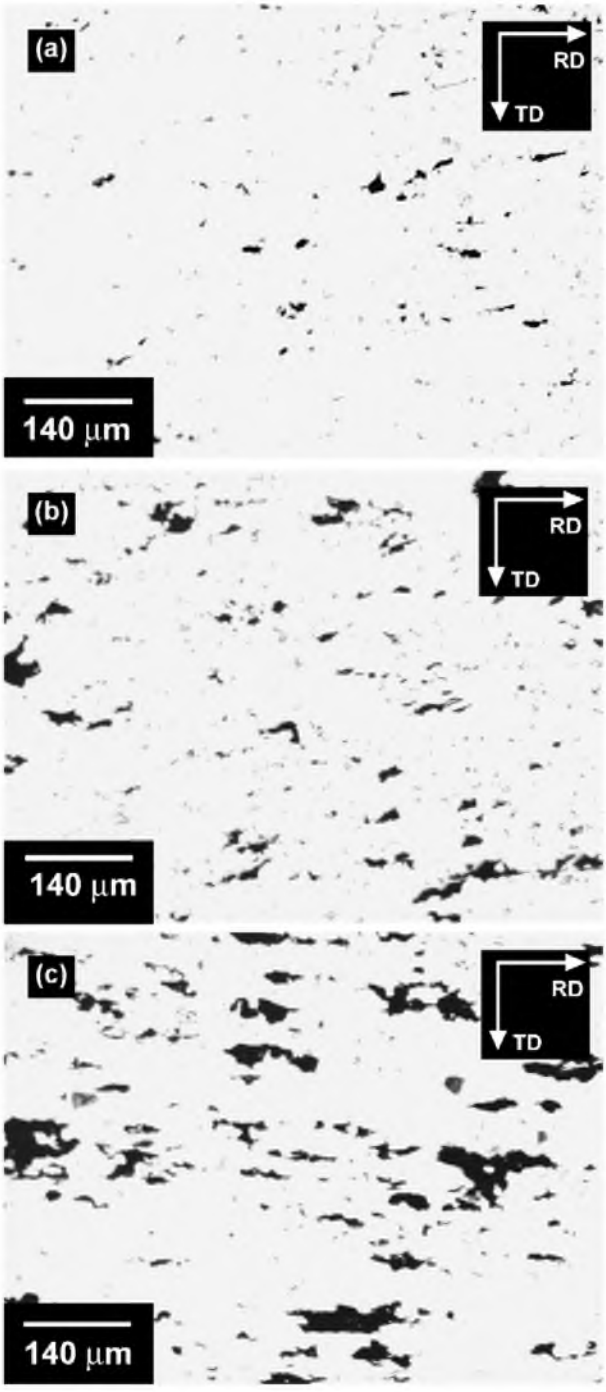

Fig. 10. Cross-sectional views of samples deformed at $1.4 \times 10^{-3}\,s^{-1}$. (a) $T = 400$ °C, $\varepsilon = 1.8$; (b) $T = 425$ °C, $\varepsilon = 2.1$ and (c) $T = 450$ °C, $\varepsilon = 1.9$.

continuous one (CSRX) during heating before deformation. It was recently shown [18] that CSRX can occur in fine-grained aluminum alloys in which the fraction of HAGBs is >64% as in the present case. At a fraction of HAGBs <62%, DSRX takes place resulting in non-uniform structure [18] as it was observed in the 7055 Al subjected to only ECAE [13] or conventional TMP [12]. Therefore, an increment in the fraction of deformation-induced HAGBs, which resulted from IR following ECAE, provides the formation of uniform fine grained structure in the 7055 Al under superplastic conditions. It is seen in Fig. 9b and Table 1 that 400 °C is a point at which CSRX starts to occur in the present 7055 Al, resulting in a roughly uniform microstructure before deformation. It is concluded, therefore, that the role of IR following ECAE is as follows:

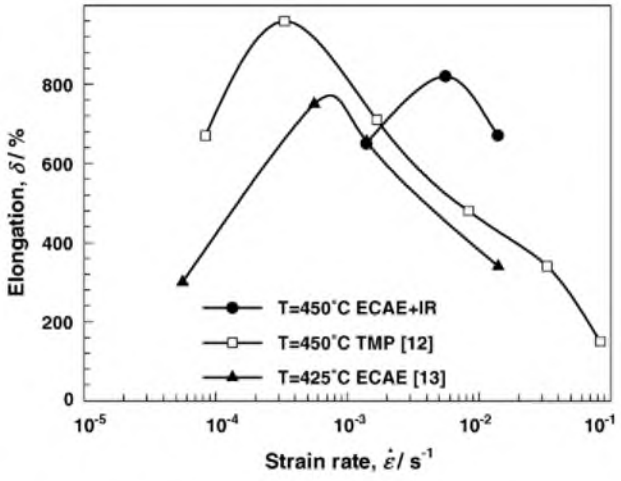

Fig. 11. Elongation to failure as a function of strain rate at optimum temperatures of superplasticity for three different states of 7055 Al.

(i) IR provides an increased uniformity of fine-grained structure developed by ECAE, resulting in enhancement of superplastic properties;
(ii) IR following ECAE is an economically efficient method for the mass fabrication of thin sheets with ultrafine-grained 7055 Al.

Superior superplastic behavior of the 7055 Al processed by ECAE and subsequent IR, compared to those of the alloy processed by ECAE [13] or TMP [12], is caused by the formation of a more uniform microstructure after static annealing. This leads to a shift of the optimum strain rate for superplasticity, at which highest superplastic ductilities appear; towards higher strain rates in comparison with those for conventional TMP [12] or the ECAE [13] processed 7055 Al, as shown in Fig. 11. The optimum strain rate in the present alloy is higher by a factor of 10 comparing with those for previous works (Fig. 11) [12,13] at the same temperature. It is worth noting that experimental datum point for the ECAE processed 7055 Al [13] are depicted at a temperature of 425 °C (Fig. 11) whereas ductilities of the two other states of 7055 Al are reported for 450 °C. However, at 425 and 450 °C, the optimum strain rate for superplasticity, at which the highest m value appears, for the ECAE processed 7055 Al is similar (Fig. 5b from work [13]).

It should be noted that the plastic flow starts at lower applied stresses in the 7055 Al subjected to ECAE and subsequent IR in comparison with those for the alloy subjected to TMP [12] or ECAE [13] (Fig. 4). Static annealing of the present alloy at $T \geq 400$ °C produces equiaxed grain structures with grain sizes below 10 μm (Fig. 9b, Table 1). This microstructure is suitable for frequent operation of GBS during superplastic deformation. Thus, a more uniform fine-grained structure of the 7055 Al subjected to ECAE and subsequent IR can result in apparent steady-state flow at lower flow stress comparing with that of the ECAE processed alloy [13]. In contrast, static annealing resulted in non-uniform microstructure in the TMP and ECAE processed alloys even at temperatures of superplastic deformation [12,13]. The operation of GBS in the regions of recovered subgrains requires increased flow stress [19]. This is caused by the fact that the continuity between the sliding subgrain boundaries is achieved by the generation and absorption of lattice dislocations [20]. As a result, an extensive strain hardening takes place initially before almost full formation of HAGBs along which GBS occurs [14]. It is concluded, therefore, that the steady-state flow in the superplastic 7055 Al is associated with slow grain growth during superplastic deformation, and the well-defined stress peak can be attributed to dynamic recrystallization resulting in the conversion of the partially recrystallized structure into a fully recrystallized one [14].

5. Conclusions

1. It was found that a two-step process consisting of ECAP and subsequent isothermal rolling (IR) is highly useful for the formation of uniform ultra-fine grained structure in sheets of conventional 7055 Al.
2. IR following ECAE increases the fraction of HAGBs in the final structure, providing a uniform grain structure under static annealing before hot deformation.
3. The 7055 Al alloy subjected to ECAE followed by IR exhibits some high strain rate superplasticity, with moderate tensile elongation of about 670%, and a corresponding strain rate sensitivity coefficient of 0.44 being found for a strain rate of $1.4 \times 10^{-2}\ s^{-1}$ and a temperature of 450 °C. The maximum elongation-to-failure of 820% was found at a similar temperature and an initial strain rate of $5.6 \times 10^{-3}\ s^{-1}$ with a strain rate sensitivity coefficient of about 0.6.

Acknowledgments

This work was supported, in part, by the International Science and Technology Center under Project no. 2011, and the Russian Foundation of Basic Research under Grant no. 02-02-39001.

References

[1] A.J. Barnes, Mater. Sci. Forum. 170–172 (1994) 701.
[2] J. Pilling, N. Ridley, Superplasticity in Crystalline Solids, The Institute of Metals, London, 1989.
[3] O.A. Kaibyshev, Superplasticity of Alloys, Intermetallics and Ceramics, Springer-Verlag, Berlin, 1992.
[4] Z. Horita, M. Furukawa, M. Nemoto, A.J. Barnes, T.G. Langdon, Acta Mater. 48 (2000) 3633.
[5] S. Lee, A. Utsunomiya, H. Akamatsu, K. Naishi, M. Furukawa, Z. Horita, T.G. Langdon, Acta Mater. 50 (2002) 553.
[6] F. Musin, R. Kaibyshev, Y. Motohashi, G. Itoh, Metall. Mater. Trans. A 35A (2004) 2383.

[7] F. Musin, R. Kaibyshev, Y. Motohashi, T. Sakuma, G. Itoh, Mater. Trans. 43 (2002) 2370.
[8] K.T. Park, H.J. Lee, C.S. Lee, W.J. Nam, D.H. Shin, Scr. Mater. 51 (2004) 479.
[9] H. Akamatsu, T. Fujinami, Z. Horita, T.G. Langdon, Scr. Mater. 44 (2001) 759.
[10] M. Kamachi, M. Furukawa, Z. Horita, T.G. Langdon, Mater. Sci. Eng. A361 (2003) 258.
[11] I.N. Fridlyander, Met. Sci. Heat Treat. 1 (2001) 5.
[12] R. Kaibyshev, T. Sakai, F. Musin, I. Nikulin, H. Miura, Scr. Mater. 45 (2001) 1373.
[13] R. Kaibyshev, T. Sakai, I. Nikulin, F. Musin, A. Goloborodko, Mater. Sci. Technol. 19 (2003) 1491.
[14] R. Kaibyshev, A. Goloborodko, F. Musin, I. Nikulin, T. Sakai, Mater. Trans. 43 (2002) 2408.
[15] F.J. Humphreys, P.B. Prangnell, J.R. Bowen, A. Gholinia, C. Harris, Phil. Trans. R. Soc. Lond. 357A (1999) 1663.
[16] A. Belyakov, T. Sakai, H. Miura, K. Tsuzaki, Phil. Mag. A 81 (2001) 2629.
[17] Z.Y. Ma, R.S. Mishra, Acta Mater. 51 (2003) 3551.
[18] H. Jazaeri, F.J. Humphreys, Acta Mater. 52 (2004) 3251.
[19] X. Yang, H. Miura, T. Sakai, Mater. Trans. 43 (2002) 2400.
[20] L.M. Dougherty, I.M. Robertson, J.S. Vetrano, Acta Mater. 51 (2003) 4367.